DOI: 10.1002/cbic.200700007

A Fluorogenic Peptide Containing the Processing Site of Human SARS Corona Virus S-Protein: Kinetic Evaluation and NMR Structure Elucidation

Ajoy Basak,*[a] Abhijit Mitra,[b] Sarmistha Basak,[a] Carolyn Pasko,[a] Michel Chrétien,[a] and Pamela Seaton[c]

Human severe acute respiratory syndrome coronavirus (hSARS-CoV) is the causative agent for SARS infection. Its surface glycoprotein (spike protein) is considered to be one of the prime targets for SARS therapeutics and intervention because its proteolytic maturation by a host protease is crucial for host–virus fusion. Using intramolecularly quenched fluorogenic (IQF) peptides based on hSARS-CoV spike protein (Abz-^{755}Glu-Gln-Asp-Arg-Asn-Thr-Arg-Glu-Val-Phe-Ala-Gln^{766}-Tyx-NH_2) and in vitro studies, we show that besides furin, other PCs, like PC5 and PC7, might also be involved in this cleavage event. Through kinetic measurements with recombinant PCs, we observed that the peptide was cleaved efficiently by both furin and PC5, but very poorly by PC7. The cleavage could be blocked by a PC-inhibitor, α1-PDX, in a dose-dependent manner. Circular dichroism spectra indicated that this peptide possesses a high degree of sheet structure. Following cleavage by furin, the sheet content increased, possibly at the expense of turn and random structures. ^{1}H NMR spectra from 2D COSY and ROESY experiments under physiological buffer and pH conditions indicated that this peptide possesses a structure with a turn at its C-terminal segment, close to the cleavage site. The data suggest that the cleavable peptide bond is located within the most exposed domain; this is supported by the nearby turn structure. Several strong to weak NMR ROESY correlations were detected, and a 3D structure of the spike IQF peptide that contains the crucial cleavage site R$^{761}\downarrow$E has been proposed.

Introduction

Human severe acute respiratory syndrome (hSARS)—the first major new infectious disease of this century—is unusual in its high mortality and infectivity rates. It is an acute respiratory illness that is caused by infection with the human SARS corona virus (hSARS-CoV), and probably originates from a wild reservoir. It is a novel corona virus that is related to other previously documented corona viruses, which are largely confined to domestic and other animal species.[1–4] It has now crossed the species barrier with a new variant form. The spread of this new extremely virulent SARS virus infection in humans led to the first global pandemic of the 21st century, during which over 8000 people became infected and more than 900 died. Intense research led to the complete genome sequence of SARS-CoV within six months of it being reported.[5,6] As a prevention strategy for SARS infection, attention has been drawn to the development of an effective vaccine for the virus,[7] but it is also necessary to have therapeutic options available for those who have already been infected. Currently, there is no treatment available for this rapidly spreading infection. Normally, patients who have contracted this syndrome are administered common antiviral drugs with minimal or no results, and are kept in isolation or quarantine. Research during the past three years has indicated that among many targets, the fusogenic envelope glycoprotein of SARS-CoV, also called spike (S) protein, is a major target for therapy.[8–10] Spike protein mediates viral fusion and the delivery of the viral genome into the host cell. Consequently, a S protein-targeted approach, when applied at the initial stage of infection is likely to reduce infection within and beyond the respiratory organs. We recently reported[11] that S protein is proteolytically processed by membrane-bound furin, a member of mammalian subtilase proprotein convertases (PCs).[12,13] This cleavage occurs at the RNTR$^{761}\downarrow$EV site,[11] and leads to the formation of two mature fragments: N-terminal S1 and C-terminal S2 (Figure 1); each fragment has

[a] *Prof. A. Basak, Dr. S. Basak, C. Pasko, Dr. M. Chrétien*
Hormone, Growth, and Development Program
Regional Protein Chemistry Center, Ottawa Health Research Institute
University of Ottawa, 725 Parkdale Ave., Ottawa, ON K1Y 4E9 (Canada)
Fax: (+1) 613-761-4355

[b] *Prof. A. Mitra*[+]
Department of Chemistry and Biochemistry
Manhattan College/College of Mount Saint Vincent
Riverdale, NY 10471 (USA)

[c] *Prof. P. Seaton*[+]
Department of Chemistry and Biochemistry, University of North Carolina
Wilmington, NC 28403 (USA)

[+] *These authors contributed equally to this work.*

Supporting information for this article is available on the WWW under http://www.chembiochem.org or from the author.

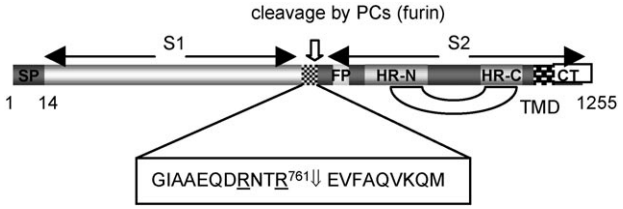

Figure 1. Schematic representation of the amino acid sequence of spike glycoprotein from human SARS corona virus and its potential site of activation. Various other characteristic functional domains are also shown; SP: signal peptide; S1 and S2: cleaved fragments of spike protein; FP: fusion peptide domain; HR-N: heptad repeat domain amino terminal; HR-C: heptad repeat domain carboxy terminal; TMD: transmembrane domain; CT: cytosolic tail; vertical double arrow: site of cleavage by PCs.

distinct biological functions. Following cleavage, S1, the globular part of S protein mediates binding to the host cell-surface receptor, angiotensin converting enzyme 2 (ACE2).[14] A 193-amino-acid segment (from residues 318–510) of S protein has been identified as the receptor-binding domain.[15] S2, a more conserved domain, forms the membrane-anchored stalk region and mediates virus–host cell fusion.[16] Ex-vivo studies with FD11 and Vero E6 cells also revealed that two other membrane-bound PCs, namely PC5B and PC7, cleave S protein; but a comparative study of their efficacies was not made either with the membrane-bound or soluble C-terminal-truncated forms. In this regard, more work is needed because these PCs have been implicated in the proteolytic maturation of a large number of other viral glycoproteins that contain a PC-recognition motif at the cleavage site.[17] In this work, we have conducted an in vitro comparative study on the cleavage of hSARS S protein with the soluble forms of furin, PC5, and PC7 by using an intramolecularly quenched model fluorogenic (IQF) peptide that was derived from the S protein cleavage site. We have also investigated the ability of a PC inhibitor to block this cleavage. Moreover, we examined the solution-phase structure of this peptide by using circular dichroism (CD) and 2D ^{1}H NMR spectroscopy studies, and have found important structural and conformational features of S protein near the crucial activation site. While CD spectroscopy[18] was used to determine the secondary structure of several SARS-CoV-derived peptides under various conditions,[19,20] NMR data[21] were more useful for determining its solution-phase structure under conditions that mimic a physiological environment.

Results

Selection of SARS-spike peptides

A number of IQF peptides based on potential PC cleavage sites of hSARS-CoV spike protein were prepared by using solid-phase Fmoc chemistry (see the Experimental Section). The location of these peptides and the various important domains of spike protein, including the heptad repeat and transmembrane domains are shown in Figure 1 by using IQF QSARS-4 as a model peptide. The chemical synthesis of IQF QSARS-4 peptide was carried out with solid-phase Fmoc chemistry and was based on various steps of repetitive Fmoc deprotections and amide couplings by using HATU and DIEA (Figure S1 A and C). In this peptide, electron transfer takes place from the donor Abz function to the acceptor nitrotyrosine moiety; this leads to the quenching of its fluorescence property (Figure S1 B). The selection of the above peptides was guided primarily by the presence of a PC sequence recognition motif, and sizes of the cleaved bands obtained in coinfection experiments with full-length hSARS-CoV spike protein and individual full-length PCs.[13] Among all of the IQF peptides tested, only QSARS-4 was found to be cleaved significantly by furin, PC5, and PC7 (vide infra), and therefore this peptide was further subjected to investigation for evaluation of its conformation and secondary structure.

In vitro digestion of QSARS-4 peptide by furin, PC5, and PC7

An initial comparative study on the digestion of QSARS-4 peptide by the soluble forms of convertases, furin, PC5 and PC7 was achieved by RP-HPLC analysis of each crude digest. Thus, it was evident that both furin and PC5, which have similar levels of enzyme activity compared to PC7 (as determined by active-site titration with the inhibitor Dec-RVKR-cmk and assay), cleave QSARS-4 peptide efficiently at the correct physiological site ($R^{761}\downarrow E$) as confirmed by mass spectra data of the HPLC peaks (Figure 2). Thus, upon cleavage QSARS-4 (Abz-^{755}Glu-Gln-Asp-Arg-Asn-Thr-Arg-Glu-Val-Phe-Ala-Gln^{766}-Tyx-NH_2; retention time (t_R) 38.4 min; M_w 1818 Da) generated two additional peaks at t_R 23.6 and 36.1 min for the N-terminal fragment (NT), Abz-Glu-Gln-Asp-Arg-Asn-Thr-Arg-OH (M_w 1036 Da) and the C-terminal fragment (CT), Glu-Val-Phe-Ala-Gln-Tyx-NH_2 (M_w 801 Da), respectively. The peak areas that correspond to the NT and CT fragments were significantly higher in furin and PC5 digests compared to PC7 digest. In fact, the intensities of these fragment peaks were very weak in the HPLC chromatogram of the PC7 digest. Based on peak heights or areas, it is estimated that about 18–25% of the peptide is cleaved by furin and PC5, and only about 1% is cleaved by PC7 under identical conditions (Figure 2, Table 1). This amount of cleavage, though small, is still considered to be significant when compared to that observed in other similar systems.[11,17,22]

Measurements of kinetic parameters, V_{max}, K_m, and K_{cat}

Michaelis–Menten plots for the determination of V_{max} and K_m for the digestion of QSARS-4 peptide by soluble recombinant furin, PC5, and PC7 are shown in Figure 3. The measured kinetic parameters are presented in Table 1. The amount of active enzyme (E_o) in each PC sample was determined with active-site titration by using the covalent inhibitor Dec-RVKR-cmk, and by assuming that each PC enzyme was inactivated in a 1:1 stoichiometric ratio, as in the case of trypsin by TLCK (tosyl lysine chloromethyl ketone).[23] Our data show that among the three soluble PCs examined, furin was the most potent enzyme in cleaving QSARS-4 at the $R^{761}\downarrow E$ site in vitro; the measured K_{cat}/K_m ratio for furin digestion was 92.4 $\mu M^{-1} h^{-1}$. This was ~2.4

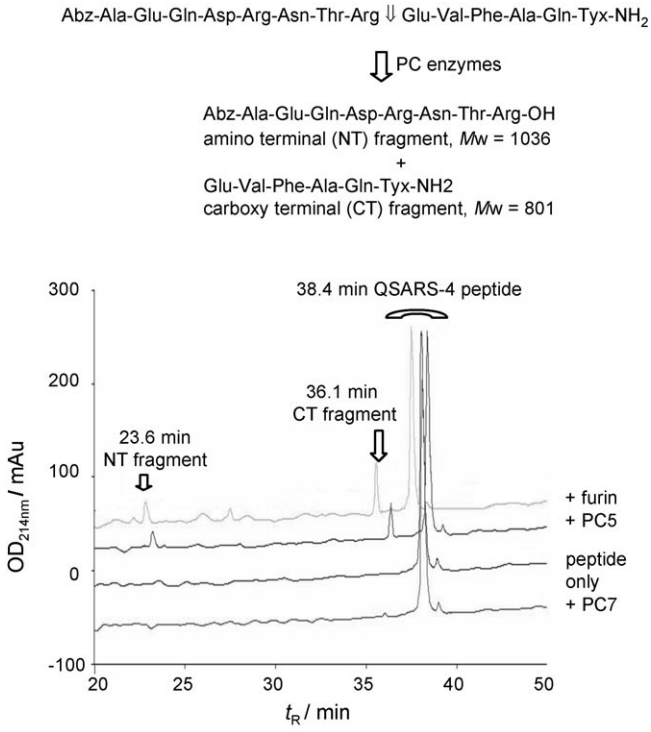

enzyme	% peptide cleaved (peak area)	% peptide cleaved (peak height)
furin	25.0	22.2
PC5	20.3	17.6
PC7	1.3	0.83
control	0	0

Figure 2. Overlay of RP-HPLC chromatograms of QSARS-4 and after 4 h digestion with furin, PC5, and PC7. The table indicates the percentage of peptide cleaved based on chromatogram peak areas or heights.

Table 1. Measured kinetic parameters and their comparisons for the cleavage of QSARS-4 peptide by soluble recombinant furin, PC5, and PC7 enzymes under identical conditions. The underlined value indicates the most potent cleavage.

Enzyme	Concentration, E_o [μM]	V_{max}, V_{max}/E_o [μM h^{-1}]	K_m [μM]	K_{cat} [h^{-1}]	K_{cat}/K_m [h^{-1} μM^{-1}]	$(K_{cat}/K_m)_{relative}$
furin	0.01082	6.03	2.64	244.0	92.4	<u>24.3</u>
PC5	0.0436	16.43	10.02	376.9	37.6	9.9
PC7	0.0886	1.64	4.86	18.5	3.8	1

and 24.3-fold better than the corresponding values for PC5 and PC7 digestions, respectively. It was further noted that the lowest K_m value was obtained with furin; this suggests a stronger interaction between the substrate and QSARS-4. Moreover, the highest K_{cat} value was obtained for PC5 and the lowest for PC7; this indicated a rapid and slow turnover for the two enzymes, respectively.

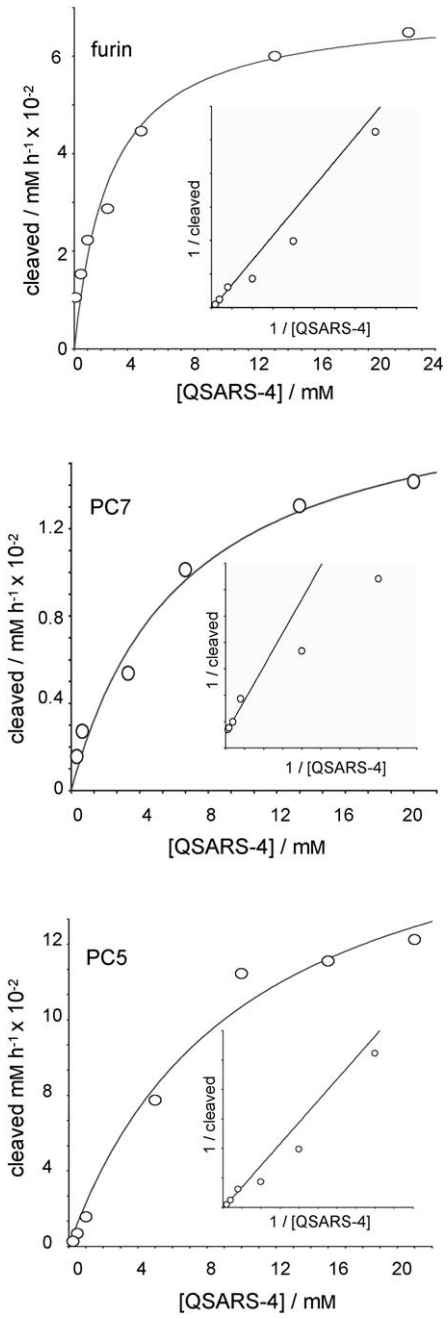

Figure 3. Michaelis–Menton plots for furin, PC5, and PC7-mediated cleavages of QSARS-4 peptide at varying concentrations.

Effect of PC inhibitor α1-PDX on QSARS-4 cleavage

When QSARS-4 (40 μg) was digested with furin (0.2 U μL^{-1}) for 2 h in the presence of increasing amounts of PC inhibitor, α1-PDX,[22] cleavage gradually diminished. This was confirmed by the gradual decrease in peak intensity of the CT-cleaved fragment (t_R = 47.5 min) in the RP-HPLC chromatogram as the amount of PC inhibitor α1-PDX gradually increased from 0 to 10 μM (Figure 4). This suggests that α1-PDX blocked the PC-mediated cleavage of QSARS-4 peptide. The observed differences in the retention times of peptide peaks of this HPLC and that shown in Figure 2 were due to differences in the HPLC

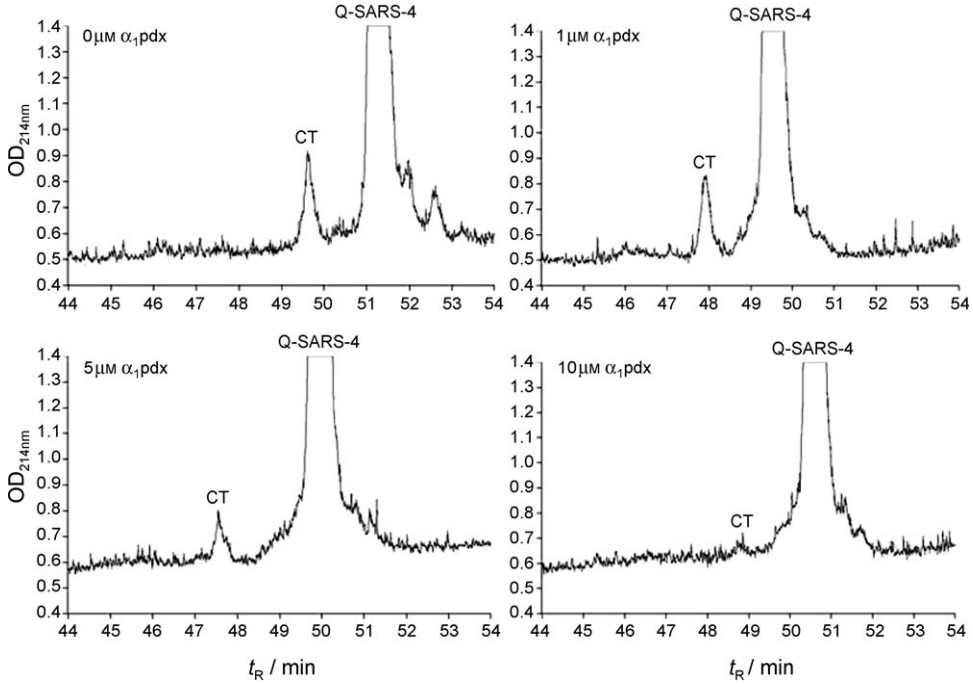

Figure 4. RP-HPLC chromatograms of furin digested QSARS-4 peptide in absence and presence of varying concentrations of α1-PDX—a potent inhibitor of furin.

column type and the gradient method that was used. It was noted that 10 μM α1-PDX was almost sufficient to block furin-mediated (0.2 U μL^{-1}) cleavage of QSARS-4 peptide (40 μg) completely over a 2 h period. The identities of the undigested and cleaved CT-fragment peptides were fully confirmed by mass spectrometry after HPLC purification.

Circular dichroism spectra

CD spectroscopy was performed on QSARS-4 peptide in aqueous medium at various concentrations to analyze the dependency of its secondary structure on concentration. As shown in Figure 5A, the overall spectral profile did not change significantly with concentration; this suggests that the secondary structure of the peptide remained largely unchanged. As expected, only the peak intensity changed with concentration. Upon software analysis of the CD spectra, it was found that there was no helical structure present in the peptide at the concentrations used. QSARS-4 possessed a predominantly β sheet structure with ~76% content at 1 μg μL^{-1}; this increased only marginally to ~80% as the concentration was decreased to 0.25 μg μL^{-1}. This occurred mostly at the expense of the random structure, which decreased from ~20 to ~15% as the concentration of QSARS-4 decreased from 1 to 0.25 μg μL^{-1}. In all of our subsequent digestion experiments, the concentration of QSARS-4 peptide was fixed at 1 μg μL^{-1} because the CD spectra at this concentration were strong enough for a good structural evaluation. Upon digestion of QSARS-4 (1 μg μL^{-1}) for 30 min with increasing amounts of furin, the sheet content increased slightly, mainly at the expense of turn structures, and then remained more or less constant (Table 2). This was also displayed in overlay CD spectra (Figure 5B). Even when the incubations were performed for a longer period of time, such as 4 h, not much change was noticed in the CD spectra. Thus, the most significant change occurred immediately following initial contact with furin. Further addition of furin did not seem to alter the CD spectra to any significant extent. The CD spectra shown in Figure 5A or 5B were the net spectra that were obtained following the subtraction of the appropriate control spectra. Our data indicate that even after a long period of digestion (4 h), the mixture of undigested QSARS-4 and its cleaved fragments still exhibited a predominantly sheet structure. The presence of a high sheet content in the peptide, as found by the CD studies was not in full agreement with the NMR results (vide infra) possibly because of the differences in the peptide concentrations, and other differing conditions that were used in the two studies (see the Experimental Section).

Peptide NMR assignments and correlations

The protons of each amino acid were assigned based on analysis of COSY, HSQC, TOCSY, and ROESY spectra. Aromatic protons were assigned based primarily on COSY correlations. Although sometimes there were partial overlaps among individual peptide protons and the protons of the buffer, all amino acid protons could be assigned from their TOCSY patterns. The positions of various α, β, γ, δ, aromatic and backbone NH amide protons are shown in Figure S2 in the Supporting Information. The amide α-proton of N-terminal glutamic acid (E1) was assigned to 8.56 ppm based on a ROESY correlation between this and the Abz aromatic *ortho*-proton, to the glutamic acid amide (NH) proton (Figure S3 in the Supporting Information). Due to the similarity of TOCSY patterns (Figure S4 in the Supporting Information) for the spin systems that originate from the amide protons at 8.56 and 8.49 ppm, these two amino acids were assigned as glutamic acids E1 and E8, respectively. Analogously, the two-spin systems that originate from the amide protons at 8.19 and 8.05 ppm were assigned as glutamines Q2 and Q12. The two glutamines (Q1 and Q12) and two arginines (R4 and R7) were distinguished based on ROESY correlations between the amide and α-protons of the neighboring amino acids (Figure S5 in the Supporting Information). In addition to the assignments of all the amino-acid protons, ROESY correlations between neighboring or distant

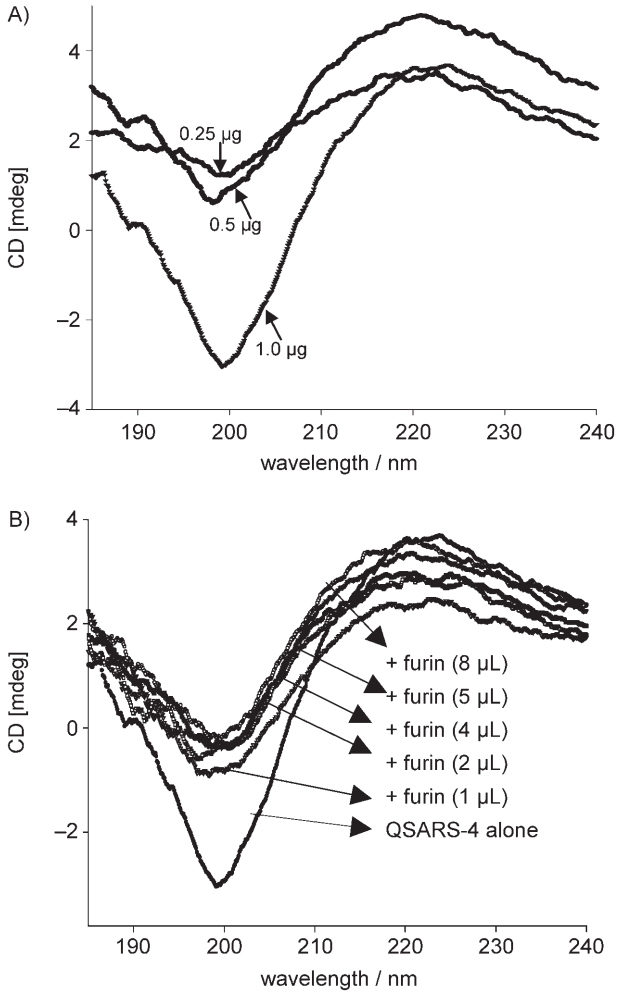

Figure 5. A) Overlay of CD spectra of QSARS-4 peptide in water at various concentrations. B) Overlay of CD spectra of QSARS-4 peptide in water following 30 min incubation with or without various amounts of recombinant furin enzyme.

Table 2. Effect on the secondary structure of QSARS-4 peptide following incubation with increasing amounts of soluble recombinant furin enzyme. Fh: frequency of helix, Fb: frequency of β-pleated sheet, Ft: frequency of turn, and Fr: frequency of random structures.

Amount of furin [µL]	Incubation time	Fh [%]	Fb [%]	Ft [%]	Fr [%]
0	30 min	0	76	5	19
1	30 min	0	87.8	1	11.2
2	30 min	0	85	2.5	12.5
4	30 min	0	86	1	13
8	30 min	0	85	2.5	12.5
0	4 h	0	76	5.5	18.5
1	4 h	0	77.3	4.3	18.4
2	4 h	0	81	4.3	14.7
4	4 h	0	77.5	5	17.5
8	4 h	0	81	4	15.3

amino acids are also listed in Figure 6, and are indicated by arrows between the interacting protons. Although there was significant overlap between some of the contours, based on

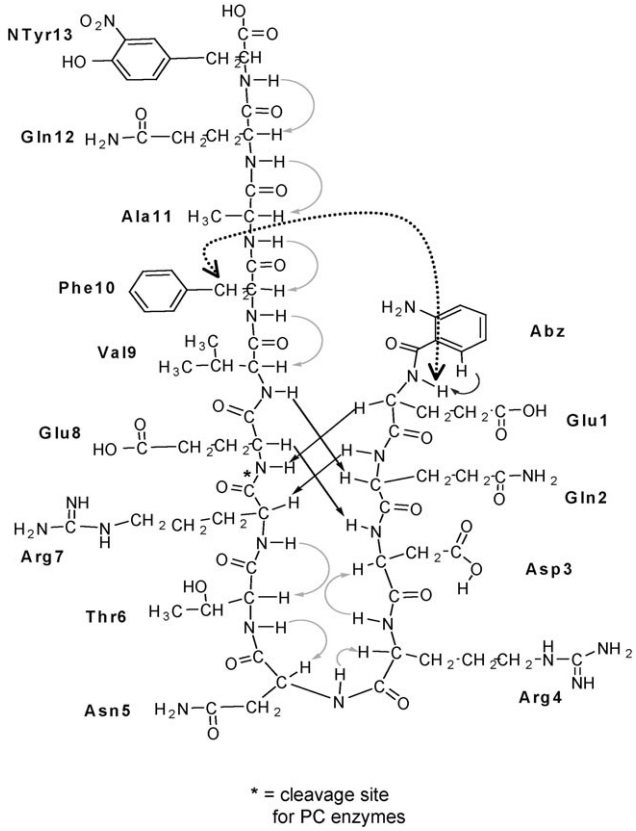

Figure 6. Proposed secondary structure of QSARS-4 peptide based on NMR data. All ROESY correlations are indicated by specific lines. Curved solid lines indicate correlations between neighboring amino acids, solid straight lines show long-range interactions. The dotted bent line shows week correlations between the amide NH of glutamic acid-1 (E1) and β-H of phenyl alanine-10 (F10). The asterisk indicates the PC-cleavage site.

the above assignments, ROESY correlations between 1) E1 and E8, 2) Q2 and V9 and E8, and 3) E8 and D3 indicate the presence of a bend in the peptide (Figure 6). Additionally, there was a very small ROESY correlation (Figures S3–S5 in the Supporting Information) between the NH of C-terminal glutamic acid (E1) and one of the β-protons of phenylalanine (F10), which provides further evidence for a bend in the peptide.

Discussion

Based on RP-HPLC analysis of crude digests and measured kinetic parameters, it was observed that QSARS-4 peptide was cleaved efficiently by both soluble furin and PC5 forms at the correct physiological $R^{761}\downarrow E$ site. Soluble PC7 also cleaved the peptide, but with very poor efficiency. This was reflected in the very low K_{cat}/K_m value for PC7 compared to those for furin and PC5. Interestingly, the K_{cat} and K_m values were high for PC5 cleavage compared to furin cleavage, but the overall catalytic efficiency of furin based on the K_{cat}/K_m ratio was nearly 2.5-fold better than that for PC5. These in vitro results indicate that PC5 and furin are the major host candidate enzymes involved in QSARS-4 cleavage.

In order to further study the kinetics and specificity of the above-described digestions experiments were performed to examine the effect of a PC inhibitor on QSARS-4 peptide cleavage. Our data show that cleavage could be blocked in vitro in a dose-dependent manner by α1-PDX—a known potent furin and PC inhibitor. α1-PDX is a bioengineered variant of α1-antitrypsin (AT) the cleavage sequence for which (AIPM^{382}) was mutated to RIPR^{382} to mimic the PC/furin recognition motif. Several studies have demonstrated the ability of α1-PDX to block proteolytic events mediated by PCs, including furin, in both in vitro and in vivo models.[22, 24–27] These proteolytic events play a crucial role in tumorigenesis, cancer metastasis, obesity, bacterial, and viral infections. Therefore, PC inhibitors are likely to find important biochemical and therapeutic applications in some of these metabolic conditions. However, further studies with full-length spike protein will be needed to examine its potential application in the study of SARS infection. Our previous study demonstrated that the other PC inhibitor, Dec-RVKR-cmk[11] is able to diminish SARS viral infectivity in Vero E6 cell lines. In this regard, it will be of great interest to study and compare the ability of various other PC inhibitors, including small peptide and nonpeptide molecules[28] to suppress SARS S protein processing and its consequences.

Our CD data suggest that the QSARS-4 peptide, which contains the crucial SARS-CoV spike protein cleavage site (RNTR^{761}↓EV) possesses a largely β-sheet structure with few turn and random structures. Even though it is an in vitro assessment based on a model peptide, this study will be valuable for future investigation of the 3D crystal structure of full-length S protein. In order to establish the relevance of our observations to physiological events, a theoretical analysis of the secondary structure of several segments of the hSARS spike protein were performed by using software (Peptide Companion) as well as web-based programs (http://www.expasy.ch). These segments were selected from regions 731–800, 741–790, 751–780, and 721–810 of S protein, all of which contain the sequence 755–766 that comprises QSARS-4 peptide. Based on the Chou–Fasman conformational parameters for these polypeptides, it is predicted that there is a turn conformation within the ^{757}DRNT^{760} segment, with a high conformation potential (magnitude 1.23). There is no preferred type of structure directly next to the turn on either side, although a few sheet and helical regions up- and downstream were noted. These structural predictions around the cleavage region were consistent with the measured CD and ^{1}H NMR data.

This study showed that the relative content of the β sheet structure can be useful for monitoring the cleavage of QSARS-4. After 30 min incubation with enzyme the β sheet content of the peptide increased only slightly; however, after an extended period of time the percentage of β sheet structure decreased. This suggests that as furin binds to QSARS-4 prior to cleavage, it promotes a structure with more β sheet content. In contrast, as furin cleaved the peptide, there was overall less β sheet structure. Even though these changes are small, they are still significant.

Our NMR data suggest that the QSARS-4 peptide was mostly linear with a possible β turn at the N terminus. This structure is most likely stabilized by the participation of hydrogen bonds between several residues at the N terminus. These include the amino acid residues around the cleavage site, as indicated in the sequence Glu-Gln-Asp-Arg-Asn-Thr-Arg^{761}↓Glu; the underlined residues indicate the exact region of the turn. Thus, the crucial P4 Arg^{758} residue is situated in the turn structure while the other critical P1 Arg^{761} residue is present immediately following the turn structure. Many short and long-distant proton–proton interactions that were shown by NMR spectroscopy (Figure 6 and Supporting Information) support this structure. It is likely that these and other close-range interactions help to stabilize the proposed structure around the cleavage site of S protein.

It is important to point out that because of the similarities between the SARS glycoprotein processing and those of HIV,[29] H5N1 type avian,[17] Ebola,[17] and Chickungunya viruses,[30] these viral glycoproteins might also possess similar structural features at their cleavage sites. Studies are in progress in our laboratory to investigate this hypothesis.

Conclusions

The present in vitro study with a model fluorogenic spike peptide confirms the crucial role of host proprotein convertases furin and PC5 in the cleavage of hSARS-CoV S protein; this leads to the formation of two functionally active distinct fragments: S1 and S2. The study also revealed that PC5 is almost as effective as furin in cleaving the peptide, but PC7 is not likely to be involved in this proteolytic event. It was also demonstrated that the cleavage could be blocked in a dose-dependent manner by α1-PDX. A NMR study under near physiological pH conditions showed the possible presence of a β turn in close proximity to the cleavage site. This type of secondary structure could represent a unique common feature of most viral glycoprotein processing by host PCs. To the best of our knowledge, this is one of the first attempts to demonstrate the presence of a specific secondary structure near the cleavage site by NMR and CD studies. Further studies with other viral glycoproteins will be required to confirm the general applicability of this hypothesis. The concept that SARS intervention might be feasible with PC or furin inhibitors is challenged by several observations that furin cleavage of the glycoprotein of the related Ebola virus is not important for in vitro infectivity and function.[31,32] This raises questions about the therapeutic potentials of furin inhibitors in SARS infection.

Experimental Section

General: All Fmoc (fluorenyl methoxy carbonyl) L-amino acids, resins such as Fmoc-PAL-PEG-PS resin (polyamide linker polyethylene glycol polystyrene; PAL: 5-[4-fmoc-aminomethyl-3,5-dimethoxy-phenoxy] valeric acid), solvents, coupling reagents, like HATU (*O*-hexafluorophospho-[7-azabenzotriazol-1-yl]-*N,N,N′,N′*-tetramethyluronium) and DIEA (diisopropyl ethyl amine), and TFA (trifluroacetic acid) were purchased from Novabiochem-Calbiochem (San Diego, CA, USA), ChemImpex International (Wood Dale, IL, USA), Applied Biosystems Inc (Framingham, MA, USA), and Bachem Inc. (King of Prussia, PA, USA). Energy absorbing matrices for MALDI-

TOF mass spectrometry, namely CHCA (α-cyano-4-hydroxycinnamic acid) and DHB (1,2-dihydroxybenzoic acid) were purchased from Aldrich Chemical Co. (Milwaukee, WI, USA). Peptide standards for the calibration of mass spectra were purchased from Sigma Chemical Co. (St. Louis, MO, USA). The furin inhibitors, α1-PDX and decanoyl (Dec)-RVKR-cmk (chloromethyl ketone) were purchased from ABR-Affinity BioReagents (Golden, CO, USA). The fluorogenic substrate Boc-RVKR-MCA (MCA: 4-methyl coumarin-7-amide) and free AMC (7-amino-4-methylcoumarin) were purchased from Bachem Inc.

Peptide synthesis and purification: Five intramolecularly quenched fluorogenic peptides based on potential PC-cleavage sites of SARS-CoV S protein, were selected. These were QSARS-1$^{789-802}$: **Abz**-^{789}Pro-Asp-Pro-Leu-Lys-Pro-Thr-Lys-**Arg**^{797}**?**Ser-Phe-Ile-Glu-Asp^{802}-**Tyx**-Ala; QSARS-2$^{439-451}$: **Abz**-^{439}Lys-Tyr-**Arg**-Tyr-Leu-**Arg**^{444}**?** His-Gly-Lys-Leu-**Arg**^{449}**?**Pro-Phe451-**Tyx**-Ala; QSARS-3$^{177-188}$: **Abz**-^{177}Gly-Asn-Phe-**Lys**-His-Leu-**Arg**^{183}**?**Glu-Phe-Val-Phe-Lys^{188}-**Tyx**-Ala; QSARS-4$^{755-766}$**: Abz**-^{755}Glu-Gln-Asp-Arg-Asn-Thr-Arg^{761}↓Glu-Val-Phe-Ala-Gln^{766}-**Tyx**-Ala; and QSARS-5$^{93-104}$: **Abz**-^{93}Glu-**Lys**-Ser-Asn-Val-Val-**Arg**^{99}**?**Gly-Trp-Val-Phe-Gly^{104}-**Tyx**-Ala. The vertical arrow (↓) is the confirmed cleavage site whereas the question marks (?) indicate potential or possible cleavage sites, bold and underlining represent unnatural and basic amino acids, respectively. Synthesis of all IQF peptides was accomplished on Fmoc-PAL-PEG polystyrene solid support by using an automated peptide synthesizer (Pioneer, PE-PerSeptive Biosystems, Framingham, MA, USA), following HATU/DIEA-mediated Fmoc chemistry.[13,27] For each coupling step an extended cycle (30 min) was used. After the complete synthesis, peptides were cleaved and fully deprotected from the resin as described previously.[13,27] Crude peptides were purified by RP-HPLC on a Rainin Dynamax instrument equipped with SD-1 pump by using a 300 Å C18 column (Jupiter, Phenomenex), first semipreparative column (size: 1×25 cm) followed by analytical column (size: 0.46×25 cm). The buffer system comprised an aqueous TFA (0.1%, *v/v*) solution and an organic phase of CH_3CN, which also contained TFA (0.1%, *v/v*). Peptides were eluted with a 1% min^{-1} linear gradient (5–60%) of 0.1% aqueous TFA/CH_3CN at a flow rate adjusted to 1 mL min^{-1} (for analytical run) or 2 mL min^{-1} (for semipreparative run), following a 5 min isocratic at 5% of 0.1% TFA/CH_3CN. Peaks were detected by UV absorbency (optical density measured at 214 nm), collected, lyophilized, and analyzed by MALDI-TOF mass spectrometry; amino acid analysis and N-terminal microsequencing was carried out to determine peptide identities.

Amino acid analysis: Amino acid analysis was performed by hydrolysis of each purified peptide (10–20 nmol) with HCl (6 N; 100 μL) in a sealed tube at 110 °C under vacuum for 24 h, followed by ion chromatography (Dionex, Oakville, ON, Canada) as described in reference [33]. For the detection of the two unnatural amino acids Abz and Tyx, authentic samples were used as standards to confirm their exact elution time in the chromatogram.

N-terminal microsequencing: N-terminal microsequencing of each purified peptide was conducted by using Edman degradation on a Procise instrument (Applied Biosystems, Foster City, CA, USA). Typically 250–1000 pmol of each peptide was used for analysis, and information about the full amino-acid sequence was obtained. For the two unnatural amino acids Abz and Tyx, authentic samples were used as standards along with the mixtures of all natural amino acids.[33]

Mass spectra measurement: MALDI-TOF MS were performed with a Voyager DE pro (PE Biosystem Inc, Framingham, MA, USA) instrument by using 1–2 μL of each sample and saturated CHCA or DHB[34] as an energy-absorbing matrix.

Source of enzyme and active-site titrations: The soluble truncated form of recombinant human furin (hfurin; M_W ~57 kDa, enzyme activity 2 U per μL) was purchased from New England BioLabs (Ipswich, MA, USA). One unit of activity was defined as the amount of furin that released 1 pmol of free AMC from the fluorogenic peptide Boc-RVRR-MCA in a total reaction volume of 100 μL in one minute (1 pmol of AMC per min) at 30 °C in HEPES (100 mM; pH 7.5 at 25 °C) with TritonX-100 (0.5%), $CaCl_2$ (1 mM), and 2-mercaptoethanol (1 mM). All studies were conducted with fivefold diluted stock furin with an enzyme activity of ~0.4 U μL^{-1}. Two other soluble truncated forms of recombinant PC5A and PC7 that were used in this study were obtained from crude concentrated culture media, followed by partial purification as described previously.[17,35] Soluble PC5A and PC7 both lack transmembrane domains; soluble PC5A is 915 amino acids long and soluble PC7 is 622 amino acids long. These enzymes were appropriately diluted before use to produce nearly identical levels of enzyme activity (0.4 U μL^{-1}). The exact amount of active enzyme in each preparation was determined by active-site titration with a freshly prepared solution of Dec-RVKR-cmk in the above-mentioned buffer.[23]

Circular dichromism spectra: All CD spectra were recorded at ambient temperature (~25 °C) in water at pH 7.2 by using a Jasco-810 spectropolarimeter (Easton, MD, USA) and a 0.1 mm thick rectangular quartz cell in a total volume of 100 μL. The peptide concentration in all studies except the dose-dependent experiments was maintained at 1 μg μL^{-1}. All spectra were measured at 185–240 nm, with recordings at 0.1 nm intervals. Each spectrum was recorded at least three consecutive times, averaged, and the CD spectrum of the blank buffer was subtracted. The final spectrum was then analyzed by using CD Estima software (Softsec Program, Softwood Co., Brookfield, CT, USA) for determination of contents of various secondary structures namely α helix, β pleated-sheet, β turn, and random.[34] CD spectra were first measured for QSARS-4 peptide alone at various concentrations to examine concentration effect on secondary structures. Later, CD spectra were also measured for QSARS-4 peptide at a fixed concentration of 1 μg μL^{-1} after incubation with increasing levels of soluble recombinant furin (1–8 μL, 0.2 U activity) for 30 min or 4 h.

Digestion of IQF peptides: In vitro digestion of each peptide (20 μg) was carried at 37 °C for 4 h in buffer (100 μL) that consisted of Tris (25 mM), MES (25 mM; 2-(*N*-morpholino)ethanesulfonic acid), $CaCl_2$ (2.5 mM), pH 7.4 with soluble recombinant furin, PC5 or PC7 (2 μL, ~0.4 U μL^{-1} activity). The reaction was stopped by addition of glacial acetic acid (2 μL). Each digest was then analyzed individually by RP-HPLC on a C18 analytical column under the conditions described above, except that the rate of flow was maintained at 1 mL min^{-1}. The percentage of digestion was determined based on peak area or height by using either the formula:

$$\%digestion(area) = \frac{areaCTpeak}{areaCTpeak + areaQSARS4peak}$$

or

$$\%digestion(height) = \frac{heightCTpeak}{heightCTpeak + heightQSARS4peak}$$

For this estimation the intensity of only the CT-cleaved fragment was used because of its higher optical density.

Effect of inhibitor on furin cleavage of QSARS-4: QSARS-4 (20 μg) was digested at 37 °C for 4 h with furin (20 μL, ~0.4 U μL^{-1} activity) in the absence and presence of increasing amounts of α1-PDX (1–20 μg; without preincubation). The resulting crude digests were analyzed by using RP-HPLC and MALDI-TOF MS of each collected peak.

Determination of kinetic parameters, V_{max}, K_m, and K_{cat}: For measurements of V_{max}, K_m, and K_{cat}, each soluble enzyme (10 μL furin, PC5, or PC7, which had almost identical levels of activity) was incubated (4–8 h) with various concentrations of QSARS-4 peptide (25, 20, 15, 10, 5, 2.5, 1, 0.5, 0.25, 0.1, and 0.05 μM) in the above-mentioned buffer (100 μL) in a 96-well microtiter plate at 37 °C. The rate of hydrolysis was measured from the changes in fluorescence intensity, and values were transformed into μmol h^{-1} of peptide cleaved by using standard curve and quenching corrections.[36] Data were collected in duplicates, and each value was the mean of three independent experiments; V_{max}, K_m, and K_{cat} were then calculated as described.[17,36,37] To identify the site of cleavage, each digest was analyzed with RP-HPLC by using a C18 analytical column, followed by MALDI-TOF mass spectrometry of each isolated peak. Consistent with earlier studies, we noted a significant intermolecular quenching of the released fluorescent material by the undigested substrate, especially at higher substrate concentrations. This was corrected for by using a standard quenching curve as described in reference [36].

NMR spectroscopy: All 1D and 2D ^{1}H NMR spectra of QSARS-4 were acquired on a Bruker Avance 600 MHz spectrometer (Bruker Biospin, Boston, MA, USA) by using inverse detection. The peptide (0.1 mM) was dissolved in buffer that consisted of Tris (25 mM), MES (25 mM), $CaCl_2$ (2.5 mM), pH 7.4, and D_2O (10%). All spectra were acquired at 298 °C by using solvent suppression techniques with the following Bruker pulse programs: COSY, cosydfesgpphm; HSQC, hsqcedetgp; TOCSY, mlevesgpph, and ROESY, roesygesgpph. TOCSY and ROESY spectra were acquired by using a spin lock and a mixing time of 70 ms and 300 ms, respectively. Assignments of all protons were made through evaluation and comparison of all 1D and 2D NMR spectra.[21,38,39]

Acknowledgements

The authors thank Dr. N. G. Seidah (IRCM, Montreal) for his interest and important discussions regarding the work. We also thank Andrew Chen (OHRI) for technical assistance in peptide synthesis and some HPLC work. We thank Dr. Ad Bax (NIDDK, NIH) for helpful discussions. We also acknowledge the expertise of Drs. Clemens Anklin and Pat Stone (Bruker Biospin) for acquiring the NMR spectra and structure analysis of QSARS-4 peptide. This work was supported by the Edith and Richard Strauss Foundation. The authors are also thankful to Protein Engineering Network of Excellence (PENCE), Canada (AB, MC) for funding the initial part of this work.

Keywords: circular dichroism · furin · NMR spectroscopy · protein structures · proteolytic cleavage

[1] T. G. Ksiazek, D. Erdman, C. S. Goldsmith, S. R. Zaki, T. Peret, S. Emery, S. Tong, C. Urbani, J. A. Comer, W. Lim, P. E. Rollin, S. F. Dowell, A. E. Ling, C. D. Humphrey, W. J. Shieh, J. Guarner, C. D. Paddock, P. Rota, B. Fields, J. DeRisi, J. Y. Yang, N. Cox, J. M. Hughes, J. W. LeDuc, W. J. Bellini, L. J. Anderson, *N. Engl. J. Med.* **2003**, *348*, 1953–1966.

[2] Y. Guan, B. J. Zheng, Y. Q. He, X. L. Liu, Z. X. Zhuang, C. L. Cheung, S. W. Luo, P. H. Li, L. J. Zhang, Y. J. Guan, K. M. Butt, K. L. Wong, K. W. Chan, W. Lim, K. F. Shortridge, K. Y. Yuen, J. S. Peiris, L. L. M. Poon, *Science* **2003**, *302*, 276–278.

[3] X. Bosch, *Lancet Infect. Dis.* **2004**, *4*, 65.

[4] The Chinese SARS Molecular Epidemiology Consortium, *Science* **2004**, *303*, 1666–1669.

[5] M. A. Marra, S. J. Jones, C. R. Astell, R. A. Holt, A. Brooks-Wilson, Y. S. Butterfield, J. Khattra, J. K. Asano, S. A. Barber, S. Y. Chan, A. Cloutier, S. M. Coughlin, D. Freeman, N. Girn, O. L. Griffith, S. R. Leach, M. Mayo, H. McDonald, S. B. Montgomery, P. K. Pandoh, A. S. Petrescu, A. G. Robertson, J. E. Schein, A. Siddiqui, D. E. Smailus, J. M. Stott, G. S. Yang, F. Plummer, A. Andonov, H. Artsob, et al., *Science* **2003**, *300*, 1399–1404.

[6] P. A. Rota, M. S. Oberste, S. S. Monroe, W. A. Nix, R. Campagnoli, J. P. Icenogle, S. Penaranda, B. Bankamp, K. Maher, M. Chen, S. H. Tong, A. Tamin, L. Lowe, M. Frace, J. L. DeRisi, Q. Chen, D. Wang, D. D. Erdman, T. C. Peret, C. Burns, T. G. Ksiazek, P. E. Rollin, A. Sanchez, S. Liffick, B. Holloway, J. Limor, K. McCaustland, M. Olsen-Rasmussen, R. Fouchier, S. Gunther, A. D. Osterhaus, C. Drosten, M. A. Pallansch, L. J. Anderson, W. J. Bellini, *Science* **2003**, *300*, 1394–1399.

[7] Y. Tsunetsugu-Yokota, K. Ohnishi, T. Takemori, *Rev. Med. Virol.* **2006**, *16*, 117–131.

[8] Q. C. Cai, Q. W. Jiang, G. M. Zhao, Q. Guo, G. W. Cao, T. Chen, *Acta Pharmacol. Sin.* **2003**, *24*, 1051–1059.

[9] B. Tripet, M. W. Howard, M. Jobling, R. K. Holmes, K. V. Holmes, R. S. Hodges, *J. Biol. Chem.* **2004**, *279*, 20836–20849.

[10] X. Xiao, S. Chakraborti, A. S. Dimitrov, K. Gramatikoff, D. S. Dimitrov, *Biochem. Biophys. Res. Commun.* **2003**, *312*, 1159–1164.

[11] E. Bergeron, M. J. Vincent, L. Wickham, J. Hamelin, A. Basak, S. T. Nichol, M. Chretien, N. G. Seidah, *Biochem. Biophys. Res. Commun.* **2005**, *326*, 554–563.

[12] N. G. Seidah, M. Chretien, *Brain Res.* **1999**, *848*, 45–62.

[13] G. Thomas, *Nat. Rev. Mol. Cell Biol.* **2002**, *3*, 753–766.

[14] W. Li, M. J. Moore, N. Vasilieva, J. Sui, S. K. Wong, M. A. Berne, M. Somasundaran, J. L. Sullivan, K. Luzuriaga, T. C. Greenough, H. Choe, M. Farzan, *Nature* **2003**, *426*, 450–454.

[15] S. K. Wong, W. Li, M. J. Moore, H. Choe, M. Farzan, *J. Biol. Chem.* **2004**, *279*, 3197–3201.

[16] P. Prabakaran, X. Xiao, D. S. Dimitrov, *Biochem. Biophys. Res. Commun.* **2004**, *314*, 235–241.

[17] A. Basak, M. Zhong, J. S. Munzer, M. Chretien, N. G. Seidah, *Biochem. J.* **2001**, *353*, 537–545.

[18] S. M. Kelly, N. C. Price, *Curr. Protein Pept. Sci.* **2000**, *1*, 349–384.

[19] P. Ingallinella, E. Bianchi, M. Finotto, G. Cantoni, D. M. Eckert, V. M. Supekar, C. Bruckmann, A. Carfi, A. Pessi, *Proc. Natl. Acad. Sci. USA* **2004**, *101*, 8709–8714.

[20] K. Yuan, L. Yi, J. Chen, X. Qu, T. Qing, X. Rao, P. Jiang, J. Hu, Z. Xiong, Y. Nie, X. Shi, W. Wang, C. Ling, X. Yin, K. Fan, L. Lai, M. Ding, H. Deng, *Biochem. Biophys. Res. Commun.* **2004**, *319*, 746–752.

[21] J. Cavanagh, W. Fairbrother, A. G. Palmer, N. Skelton, *Protein NMR Spectroscopy: Principles and Practice*, Academic Press, Philadelphia, **2002**.

[22] F. Jean, K. Stella, L. Thomas, G. Liu, Y. Xiang, A. J. Reason, G. Thomas, *Proc. Natl. Acad. Sci. USA* **1998**, *95*, 7293–7298.

[23] P. Ascenzi, G. Balliano, C. Gallina, F. Polticelli, M. Bolognesi, *Eur. J. Biochem.* **2000**, *267*, 1239–1246.

[24] Y. Cui, F. Jean, G. Thomas, J. L. Christian, *EMBO J.* **1998**, *17*, 4735–4743.

[25] D. E. Bassi, R. L. De Cicco, H. Mahloogi, S. Zucker, G. Thomas, A. J. P. Klein-Szanto, *Proc. Natl. Acad. Sci. USA* **2001**, *98*, 10326–10331.

[26] B. Bahbouhi, M. Bendjennat, D. G. Tard, N. G. Seidah, E. Bahraou, *Biochem. J.* **2000**, *352*, 91–98.

[27] G. Siegfried, A. Basak, J. A. Cromlish, S. Benjannet, J. Marcinkiewicz, M. Chretien, N. G. Seidah, A. M. Khatib, *J. Clin. Invest.* **2003**, *111*, 1723–1732.

[28] A. Basak, *J. Mol. Med.* **2005**, *83*, 844–855.

[29] D. Turner, M. A. Wainberg, *AIDS Rev.* **2006**, *8*, 17–23.

[30] I. Schuffenecker, I. Iteman, A. Michault, S. Murri, L. Frangeul, M. C. Vaney, R. Lavenir, N. Pardigon, J. M. Reynes, F. Pettinelli, L. Biscornet, L. Diancourt, S. Michel, S. Duquerroy, G. Guigon, M. P. Frenkiel, A. C. Brehin, N. Cubito, P. Despres, F. Kunst, F. A. Rey, H. Zeller, S. Brisse, *PLoS Med.* **2006**, *23*, 3–7.

[31] G. Neumann, H. Feldmann, S. Watanabe, I. Lukashevich, Y. Kawaoka, *J. Virol.* **2002**, *76*, 406 – 410.
[32] R. J. Wool-Lewis, P. Bates, *J. Virol.* **1999**, *73*, 1419 – 1426.
[33] A. Basak, F. Lotfipour, *FEBS Lett.* **2005**, *579*, 4813 – 4821.
[34] K. Beking, X. Hao, S. Basak, A. Basak, *Pept. Protein Lett.* **2005**, *12*, 197 – 202.
[35] M. Zhong, J. S. Munzer, A. Basak, S. Benjannet, S. J. Mowla, E. Decroly, M. Chretien, N. G. Seidah, *J. Biol. Chem.* **1999**, *274*, 33913 – 33920.
[36] C. Lazure, D. Gauthier, F. Jean, A. Boudreault, N. G. Seidah, H. P. Bennett, G. N. Hendy, *J. Biol. Chem.* **1998**, *273*, 8572 – 8580.
[37] K. Johanning, M. A. Juliano, L. Juliano, C. Lazure, N. S. Lamango, D. F. Steiner, I. Lindberg, *J. Biol. Chem.* **1998**, *273*, 22672 – 22680.
[38] K. Wüthrich, *NMR of Proteins and Nucleic Acids*, Wiley, New York, **1986**.
[39] R. T. Williamson, A. C. Barrios Sosa, A. Mitra, P. J. Seaton, D. B. Weibel, F. C. Schroeder, J. Meinwald, F. E. Koehn, *Org. Lett.* **2003**, *5*, 1745 – 1748.

Revised: January 5, 2007
Published online on April 30, 2007

